Journal of Control, Automation and Electrical Systems (2020) 31:1335–1347
https://doi.org/10.1007/s40313-020-00641-5

An $\mathscr{H}_\infty$ Approach to Data-Driven Offset-Free Tracking

M. Salim[1] · B. Esmaeili[1]

Received: 15 April 2019 / Revised: 18 May 2020 / Accepted: 7 September 2020 / Published online: 25 September 2020

Abstract
Data-driven controllers also called model-free controllers were invented in order to omit plant modeling step of model-based controllers. Design procedure of these controllers is directly based on experimental I/O data collected from real plant. It can ensure their reliability in real world applications, where the exact model is not available in most cases. In this paper, we consider the problem of accurate tracking performance in presence of external disturbances using data-driven methodologies combined with $\mathscr{H}_\infty$ approach. Defining the improved subspace-based predictor, as the base step of the proposed controller's design procedure, an integrator is applied to the control loop, which increases the accuracy of controller's reference tracking performance. Moreover, a weighting function is considered for disturbance attenuation. Simulation results evidently illustrate efficiency and satisfactory performance of the proposed controller.

Keywords Data-driven control · Subspace predictor · $\mathscr{H}_\infty$ control · Offset-free tracking

1 Introduction

Plant modelling is a very important step in model-based control design procedures. However, in most cases the exact model is not available due to uncertainties of plants or their nonlinear and time varying structures. Also, the process of plant modelling is expensive and the obtained model is limited for a special operating range. Therefore, the model can not represent real plant properly. According to these drawbacks, many solutions were investigated to reduce dependency of the controllers on plant model, including adaptive controllers (Khajehsaeid et al. 2019), neural-network based controllers (Ge et al. 2013), fuzzy controllers (Precup and Hellendoorn 2011) or fuzzy neural network based controllers (Esmaeili et al. 2018). Data-driven controllers have attracted the attention of researchers in recent years. A comprehensive review of aforementioned controllers and their differences with model-based ones has been presented in Hou and Wang (2013). In data-driven technique, the controller is designed directly using input/output (I/O) data of real plant, which eliminates difficulty and computational burden of model identification process and is more reliable because of stabilizing the real plant and not only the model of the system. This technique is divided into several methods such as iterative feedback tuning (Heertjes et al. 2016), virtual reference feedback tuning (Yan et al. 2016), model-free adaptive control (Esmaeili et al. 2019), and etc. But among them, subspace approach has gained great popularity in data-driven techniques (Van Overschee and De Moor 1994; Van Overschee and De Moor 1996; Houtzager et al. 2012; Markovsky et al. 2005; Katayama 2006). However, drastic computation burden of system identification step in the aforementioned studies is a disadvantage for real-time implementations. Hence, several studies have been published concerning model-free subspace-based controllers. Favoreel et al. (1999) used subspace approach for designing linear quadratic Gaussian (LQG) controller. Woodley et al. (2001) proposed a novel data-driven $\mathscr{H}_\infty$ controller in order to control unknown linear time-invariant (LTI) systems. An adaptive determination algorithm for updating subspace predictor's coefficients was presented in Woodley et al. (2001b), which has been used in Elkaim et al. (2006) and Chen et al. (2014) for robust tracking of an autonomous surface vehicle and controlling solar power system, respectively. Also, data-driven $\mathscr{H}_\infty$ methodology has been used in fault tolerant control (Hallouzi and Verhaegen 2008) and simultaneous fault detection and controller design procedure in Salim and Khosrowjerdi (2016) and Salim and Khosrowjerdi (2017), respectively.

✉ M. Salim
m.salim@tabrizu.ac.ir

[1] Control Engineering Department, Faculty of Electrical and Computer Engineering, University of Tabriz, Tabriz 5166616471, Iran

One of the most important objectives in control is accurate and offset-free tracking performance, which is crucial for real-world applications such as motion control systems (linear-motor control, permanent-magnet motor control and etc.), industrial processes (PH neutralization control, liquid level control, temperature control, injection molding process control and etc.), and its loss may cause unsatisfactory closed-loop performance and also waste the controller's design cost. The major drawback of the aforementioned studies is their less tracking accuracy. In the literature, forcing an integral action into the control design procedure is one of the most common methods for both model-based and data-driven control fields. This method has been used in model-based predictive controllers (MPC) (Cheng et al. 2015; Li et al. 2016), subspace based predictive controllers (Kadali et al. 2003; Wahab et al. 2011; Lu et al. 2011; Wu et al. 2014; Lu et al. 2015; Shafiei et al. 2015; Luo and Song 2018; Vajpayee et al. 2018) and feedback linearization control (Errouissi et al. 2016) in which incremental control input is determined instead of control input to reduce steady-state tracking error. Also, in sliding mode controllers, an integral term has been utilized in sliding surface to enhance the tracking performance (Esmaeili et al. 2019a; Van 2019). Up to now, offset-free tracking performance in data-driven $\mathscr{H}_\infty$ controller has not yet been studied, which motivates us to propose a data-driven offset-free $\mathscr{H}_\infty$ controller to meet control objectives, i.e., accurate reference tracking and disturbance attenuation. To the best of authors' knowledge, it is the first time that both offset-free tracking and disturbance attenuation issues are considered in data-driven $\mathscr{H}_\infty$ controller. The main contributions of this work are summarized as follows:

(1) A weight function is considered to attenuate effect of external disturbance.
(2) An integral action is imposed to the controller system using an improved subspace predictor.
(3) Since only I/O data are used for designing process of the controller, the proposed method is useful in industrial processes with unknown models.

The rest of the paper is organized as follows: Sect. 2 defines the problem of data-driven offset-free tracking as a time domain $\mathscr{H}_\infty$ optimization problem. In Sect. 3 improved subspace predictor is determined using traditional subspace predictor, which is necessary for data-driven technique. The proposed data-driven $\mathscr{H}_\infty$ offset-free controller design procedure is presented in Sect. 4. Two demonstrative examples verify the effectiveness of the proposed study in Sects. 5 and 6 concludes the paper.

2 Preliminaries and Problem Statement

For a matrix P, P^T and $\bar{\lambda}(P)$ stand for its transpose and maximum eigenvalue, respectively. Matrix P is called symmetric if $P = P^T$. For symmetric matrices P and Q, $P \geq Q$ and $P > Q$ denote $P - Q$ is positive semi definite and positive definite, respectively. I and $\mathscr{R}\mathscr{H}_\infty$ indicate unity matrix with appropriate dimension and the space of real rational, proper and stable transfer matrices, respectively.

Lemma 1 (Inversion lemma) *If A_1^{-1} and A_3^{-1} exist, then*

$$\begin{bmatrix} A_1 & A_2 \\ A_2^T & A_3 \end{bmatrix}^{-1} = \begin{bmatrix} (A_1 - A_2 A_3^{-1} A_2^T)^{-1} & -(A_1 - A_2 A_3^{-1} A_2^T)^{-1} A_2 A_3^{-1} \\ -(A_3 - A_2^T A_1^{-1} A_2)^{-1} A_2^T A_1^{-1} & (A_3 - A_2^T A_1^{-1} A_2)^{-1} \end{bmatrix} \tag{1}$$

It is worth pointing out that multiplying $\begin{bmatrix} 0 & I \end{bmatrix}$ to the left of (1) yields

$$\begin{bmatrix} 0 & I \end{bmatrix} \begin{bmatrix} A_1 & A_2 \\ A_2^T & A_3 \end{bmatrix}^{-1} = (A_3 - A_2^T A_1^{-1} A_2)^{-1} \begin{bmatrix} -A_2^T A_1^{-1} & I \end{bmatrix} \tag{2}$$

Lemma 2 (Schur decomposition) *If D is a symmetric matrix, therefore, it can be decomposed as*

$$D = \begin{bmatrix} A_1 & A_2 \\ A_2^T & A_3 \end{bmatrix} = \begin{bmatrix} I & A_2 A_3^{-1} \\ 0 & I \end{bmatrix} \begin{bmatrix} A_1 - A_2 A_3^{-1} A_2^T & 0 \\ 0 & A_3 \end{bmatrix} \times \begin{bmatrix} I & A_2 A_3^{-1} \\ 0 & I \end{bmatrix}^T \tag{3}$$

In this paper, we consider a linear time-invariant system as follows

$$G : \begin{cases} x_{k+1} = A\, x_k + B\, u_k + B_d\, d_k + e_k, \\ y_k = C\, x_k + D\, u_k + D_d\, d_k + v_k \end{cases} \tag{4}$$

where $x_k \in \mathbb{R}^n$, $u_k \in \mathbb{R}^m$, $y_k \in \mathbb{R}^l$ and $d_k \in \mathbb{R}^{k_d}$ are the system states, the known input of plant, the measured output of plant and the external disturbance, respectively. Also, $e_k \in \mathbb{R}^n$ and $v_k \in \mathbb{R}^l$ are process and measurement's normally distributed, white noise sequences, respectively. System matrices A, B, B_d, C, D and D_d are supposed to be unknown and constant matrices of appropriate dimensions.

Assumption 1 The pair (A, B) is stabilizable.

Assumption 2 The pair (C, A) is detectable.

Consider healthy system, i.e., system (4) such that $d_k = 0$ and suppose that process and measurement noise sequences are integrated noises. We have:

$$\begin{cases} x_{k+1} = A\,x_k + B\,u_k + \xi_k, \\ y_k = C\,x_k + D\,u_k + \vartheta_k \end{cases} \tag{5}$$

where ξ_k and ϑ_k are integrated noises. Therefore

$$\xi_k = \xi_{k-1} + e_k = \frac{1}{\Delta} e_k \tag{6}$$

and

$$\vartheta_k = \vartheta_{k-1} + v_k = \frac{1}{\Delta} v_k \tag{7}$$

where Δ is differentiating operator. By substituting (6) and (7) into (5), one can obtain

$$\begin{cases} \Delta x_{k+1} = A\,\Delta x_k + B\,\Delta u_k + e_k, \\ \Delta y_k = C\,\Delta x_k + D\,\Delta u_k + v_k \end{cases} \tag{8}$$

which gives incremental control input Δu instead of control input u. Assume the experimental I/O data of healthy system are available. The purpose is to design a data-driven $\mathscr{H}_\infty$ controller to obtain an offset-free tracking performance while external disturbance is attenuated with a reasonable incremental control effort. Besides, the overall design process of the proposed controller is merely based on the I/O data of the controlled plant. Consequently, these objectives are augmented as the following control objective vector:

$$z_c \triangleq \begin{bmatrix} z_r \\ z_u \end{bmatrix} = \begin{bmatrix} W_r(r-y) \\ W_u \Delta u \end{bmatrix} \tag{9}$$

where W_r and W_u are proper stable weighting functions for precise tracking performance and bounded incremental control effort, respectively. Define cost function as follows:

$$J(\gamma) \triangleq \sum_{k=0}^{i-1} (z_c{}^T z_c - \gamma^2 w^T w) \tag{10}$$

where i denotes finite horizon length, γ is design parameter and $w \in \mathbb{R}^{l+k_d}$ is the exogenous input defined as follows

$$w = \begin{bmatrix} r \\ d \end{bmatrix} \tag{11}$$

where $r \in \mathbb{R}^l$ is the reference input. In order to specify r and d in terms of w, we define the following matrices

$$\begin{aligned} r &= K_1 w, \quad K_1 = \begin{bmatrix} I_l & 0_{l\times k_d} \end{bmatrix} \\ d &= K_2 w, \quad K_2 = \begin{bmatrix} 0_{k_d \times l} & I_{k_d} \end{bmatrix} \end{aligned}$$

Now, one can formulate the $\mathscr{H}_\infty$ control problem as a finite horizon min–max suboptimal problem as follows:

$$\min_{\Delta u} \sup_{w} \; J(\gamma) \le 0 \tag{12}$$

in which the optimal Δu and therefore, the optimal u is obtained such that it guarantees $\mathscr{H}_\infty$ gain from w to z be less than γ in the presence of maximum exogenous input, i.e., w. The feasibility condition of the aforementioned optimization problem and optimal solution of it will be determined in Sect. 4.

3 Improved Subspace Predictor Design

In this section, first, we briefly review design procedure of the traditional subspace predictor (Van Overschee and De Moor 1996) and then, the differentiated I/O data will be used to obtain improved version, which is a function of incremental control input Δu.

3.1 Traditional Subspace Predictor

The problem of designing traditional subspace predictor can be formulated as follows: *Consider k to be the current time step. Given past experimental data* $(W_p)_k$ *and future inputs* $\begin{bmatrix} u_k \\ \vdots \\ u_{k+i-1} \end{bmatrix}$, calculate L_u, L_w to predict future outputs of plant, namely

$$\begin{bmatrix} \hat{y}_k \\ \cdots \\ \hat{y}_{k+i-1} \end{bmatrix} = L_w (W_p)_k + L_u \begin{bmatrix} u_k \\ \vdots \\ u_{k+i-1} \end{bmatrix} \tag{13}$$

where

$$(W_p)_k \triangleq \left(\begin{bmatrix} u_{k-i} \\ \vdots \\ u_{k-1} \\ y_{k-i} \\ \vdots \\ y_{k-i} \end{bmatrix} \right) \tag{14}$$

Suppose the experimental I/O data of length N from the unknown healthy LTI system

$$\begin{cases} x_{k+1} = A\,x_k + B\,u_k + e_k, \\ y_k = C\,x_k + D\,u_k + v_k \end{cases} \tag{15}$$

is available as follows

$$\left(\begin{bmatrix} u_0 \\ u_1 \\ \vdots \\ u_{N-1} \end{bmatrix}, \begin{bmatrix} y_0 \\ y_1 \\ \vdots \\ y_{N-1} \end{bmatrix}\right) \tag{16}$$

In order to determine linear subspace predictor equation, we should define Hankel matrices from the I/O data (16) as follows:

$$U_p = \begin{bmatrix} u_0 & u_1 & \cdots & u_{j-1} \\ u_1 & u_2 & \cdots & u_j \\ \vdots & \vdots & \cdots & \vdots \\ u_{i-1} & u_i & \cdots & u_{i+j-2} \end{bmatrix} \in \mathbb{R}^{im \times j} \tag{17}$$

$$Y_p = \begin{bmatrix} y_0 & y_1 & \cdots & y_{j-1} \\ y_1 & y_2 & \cdots & y_j \\ \vdots & \vdots & \cdots & \vdots \\ y_{i-1} & y_i & \cdots & y_{i+j-2} \end{bmatrix} \in \mathbb{R}^{il \times j} \tag{18}$$

$$U_f = \begin{bmatrix} u_i & u_{i+1} & \cdots & u_{i+j-1} \\ u_{i+1} & u_{i+2} & \cdots & u_{i+j} \\ \vdots & \vdots & \cdots & \vdots \\ u_{2i-1} & u_{2i} & \cdots & u_{2i+j-2} \end{bmatrix} \in \mathbb{R}^{im \times j} \tag{19}$$

$$Y_f = \begin{bmatrix} y_i & y_{i+1} & \cdots & y_{i+j-1} \\ y_{i+1} & y_{i+2} & \cdots & y_{i+j} \\ \vdots & \vdots & \cdots & \vdots \\ y_{2i-1} & y_{2i} & \cdots & y_{2i+j-2} \end{bmatrix} \in \mathbb{R}^{il \times j} \tag{20}$$

where i denotes prediction horizon, which should be chosen larger than the expected order of plant and $j = N - 2i + 1$ is the number of prediction problems. The subscripts p and f denote past and future time, respectively. A single predictor should be found such that optimizes (in the least square sense) the j prediction problems. By solving the following Frobenius norm minimization problem, output prediction $\hat{Y}_f$ can be obtained:

$$\min_{L_w, L_u} \left\| Y_f - \begin{bmatrix} L_w & L_u \end{bmatrix} \begin{bmatrix} W_p \\ U_f \end{bmatrix} \right\|_F^2 \tag{21}$$

By performing a numerically reliable technique, i.e., QR decomposition, subspace predictor coefficients L_w and L_u can be obtained as follows:

$$\begin{bmatrix} W_p \\ U_f \\ Y_f \end{bmatrix} = R^T Q^T = \begin{bmatrix} R_{11} & 0 & 0 \\ R_{21} & R_{22} & 0 \\ R_{31} & R_{32} & R_{33} \end{bmatrix} \begin{bmatrix} Q_1 \\ Q_2 \\ Q_3 \end{bmatrix} \tag{22}$$

then

$$L = \begin{bmatrix} L_w & L_u \end{bmatrix} = \begin{bmatrix} R_{31} & R_{32} \end{bmatrix} \begin{bmatrix} R_{11} & 0 \\ R_{21} & R_{22} \end{bmatrix}^{\dagger} \tag{23}$$

where † stands for the Moore–Penrose inverse.

3.2 Improved Subspace Predictor

By following the same steps in determining traditional subspace predictor, the improved subspace predictor (Mardi and Wang 2009) can be obtained. Define Hankel matrices using differentiated data:

$$\Delta U_p = \begin{bmatrix} \Delta u_0 & \Delta u_1 & \cdots & \Delta u_{j-1} \\ \Delta u_1 & \Delta u_2 & \cdots & \Delta u_j \\ \vdots & \vdots & \cdots & \vdots \\ \Delta u_{i-1} & \Delta u_i & \cdots & \Delta u_{i+j-2} \end{bmatrix} \in \mathbb{R}^{im \times j}, \tag{24}$$

$$\Delta Y_p = \begin{bmatrix} \Delta y_0 & \Delta y_1 & \cdots & \Delta y_{j-1} \\ \Delta y_1 & \Delta y_2 & \cdots & \Delta y_j \\ \vdots & \vdots & \cdots & \vdots \\ \Delta y_{i-1} & \Delta y_i & \cdots & \Delta y_{i+j-2} \end{bmatrix} \in \mathbb{R}^{il \times j} \tag{25}$$

$$\Delta U_f = \begin{bmatrix} \Delta u_i & \Delta u_{i+1} & \cdots & \Delta u_{i+j-1} \\ \Delta u_{i+1} & \Delta u_{i+2} & \cdots & \Delta u_{i+j} \\ \vdots & \vdots & \cdots & \vdots \\ \Delta u_{2i-1} & \Delta u_{2i} & \cdots & \Delta u_{2i+j-2} \end{bmatrix} \in \mathbb{R}^{im \times j}, \tag{26}$$

$$\Delta Y_f = \begin{bmatrix} \Delta y_i & \Delta y_{i+1} & \cdots & \Delta y_{i+j-1} \\ \Delta y_{i+1} & \Delta y_{i+2} & \cdots & \Delta y_{i+j} \\ \vdots & \vdots & \cdots & \vdots \\ \Delta y_{2i-1} & \Delta y_{2i} & \cdots & \Delta y_{2i+j-2} \end{bmatrix} \in \mathbb{R}^{il \times j} \tag{27}$$

and

$$\Delta W_p = \begin{bmatrix} \Delta U_p \\ \Delta Y_p \end{bmatrix} \tag{28}$$

The improved subspace predictor is obtained by solving the following problem:

$$\min_{L_{w,\Delta}, L_{u,\Delta}} \left\| \Delta Y_f - \begin{bmatrix} L_{w,\Delta} & L_{u,\Delta} \end{bmatrix} \begin{bmatrix} \Delta W_p \\ \Delta U_f \end{bmatrix} \right\|_F^2 \tag{29}$$

Using the QR decomposition, we have:

$$\begin{bmatrix} \Delta W_p \\ \Delta U_f \\ \Delta Y_f \end{bmatrix} = R_\Delta^T Q_\Delta^T = \begin{bmatrix} R_{11,\Delta} & 0 & 0 \\ R_{21,\Delta} & R_{22,\Delta} & 0 \\ R_{31,\Delta} & R_{32,\Delta} & R_{33,\Delta} \end{bmatrix} \begin{bmatrix} Q_{1,\Delta} \\ Q_{2,\Delta} \\ Q_{3,\Delta} \end{bmatrix} \tag{30}$$

then

$$L_\Delta = \begin{bmatrix} L_{w,\Delta} & L_{u,\Delta} \end{bmatrix} = \begin{bmatrix} R_{31,\Delta} & R_{32,\Delta} \end{bmatrix} \begin{bmatrix} R_{11,\Delta} & 0 \\ R_{21,\Delta} & R_{22,\Delta} \end{bmatrix}^{\dagger} \tag{31}$$

and therefore, prediction of differentiated output is as follows:

$$\Delta \hat{Y}_f = L_{w,\Delta} \Delta W_p + L_{u,\Delta} \Delta U_f \tag{32}$$

The simplified version of (32) can be written as follows

$$\Delta \hat{y}_f = L_{w,\Delta} \Delta w_p + L_{u,\Delta} \Delta u_f \tag{33}$$

where $\Delta \hat{y}_f$ and Δu_f are as follows:

$$\Delta \hat{y}_f = \begin{bmatrix} \Delta \hat{y}_k \\ \Delta \hat{y}_{k+1} \\ \vdots \\ \Delta \hat{y}_{k+i-1} \end{bmatrix}, \quad \Delta u_f = \begin{bmatrix} \Delta u_k \\ \Delta u_{k+1} \\ \vdots \\ \Delta u_{k+i-1} \end{bmatrix}, \tag{34}$$

and

$$\Delta w_p = \begin{bmatrix} \Delta u_p \\ \Delta y_p \end{bmatrix} \tag{35}$$

where

$$\Delta y_p = \begin{bmatrix} \Delta y_{k-i} \\ \Delta y_{k-i+1} \\ \vdots \\ \Delta y_{k-1} \end{bmatrix}, \quad \Delta u_p = \begin{bmatrix} \Delta u_{k-i} \\ \Delta u_{k-i+1} \\ \vdots \\ \Delta u_{k-1} \end{bmatrix}$$

We can write:

$$\hat{y}_f = \begin{bmatrix} \hat{y}_k \\ \hat{y}_{k+1} \\ \vdots \\ \hat{y}_{k+i-1} \end{bmatrix} = \begin{bmatrix} \Delta \hat{y}_k \\ \Delta \hat{y}_{k+1} \\ \vdots \\ \Delta \hat{y}_{k+i-1} \end{bmatrix} + \begin{bmatrix} \hat{y}_{k-1} \\ \hat{y}_k \\ \vdots \\ \hat{y}_{k+i-2} \end{bmatrix} \tag{36}$$

Assuming that experimental I/O data are available in time step $k-1$, one can replace $\hat{y}_{k-1}$ with y_{k-1}. It yields

$$\begin{cases} \hat{y}_k = \Delta \hat{y}_k + y_{k-1} \\ \hat{y}_{k+1} = \Delta \hat{y}_{k+1} + \hat{y}_k \\ \quad \vdots \\ \hat{y}_{k+i-1} = \Delta \hat{y}_{k+i-1} + \hat{y}_{k+i-2} \end{cases} \tag{37}$$

where y_{k-1} is the plant output in previous time step. Substituting recursively $\hat{y}_k, \ldots, \hat{y}_{k+i-2}$ in the right hand-side of equations in (37) into their respective definitions on the left hand-side, we have:

$$\underbrace{\begin{bmatrix} \hat{y}_k \\ \hat{y}_{k+1} \\ \vdots \\ \hat{y}_{k+i-1} \end{bmatrix}}_{\hat{y}_f} = \underbrace{\begin{bmatrix} I_l & 0 & \cdots & 0 \\ I_l & I_l & \cdots & 0 \\ \vdots & \vdots & \cdots & \vdots \\ I_l & I_l & \cdots & I_l \end{bmatrix}}_{\Lambda_l} \underbrace{\begin{bmatrix} \Delta \hat{y}_k \\ \Delta \hat{y}_{k+1} \\ \vdots \\ \Delta \hat{y}_{k+i-1} \end{bmatrix}}_{\Delta \hat{y}_f} + \underbrace{\begin{bmatrix} I_l \\ I_l \\ \vdots \\ I_l \end{bmatrix}}_{\Phi_l} y_{k-1} \tag{38}$$

Using (33) and (38), the improved subspace predictor is obtained as follows:

$$\begin{aligned} \hat{y}_f &= \Phi_l y_{k-1} + \Lambda_l \Delta \hat{y}_f = \Phi_l y_{k-1} + \Lambda_l L_{w,\Delta} \Delta w_p \\ &\quad + \Lambda_l L_{u,\Delta} \Delta u_f \end{aligned} \tag{39}$$

Note that in the presence of unknown external disturbance d_k, its effect is expressed with an additive term, i.e., $\Lambda_l L_{d,\Delta} \Delta d_f$, as follows:

$$\begin{aligned} \hat{y}_f &= \Phi_l y_{k-1} + \Lambda_l \Delta \hat{y}_f = \Phi_l y_{k-1} + \Lambda_l L_{w,\Delta} \Delta w_p + \\ &\quad \Lambda_l L_{u,\Delta} \Delta u_f + \Lambda_l L_{d,\Delta} \Delta d_f \end{aligned} \tag{40}$$

where $d_f = [d_k^T, d_{k+1}^T, \ldots, d_{k+i-1}^T]^T$ is the vector of future disturbances and Δd_f denotes the incremental version of it. The nature of $L_{d,\Delta}$ is not important and the additive component is compensated by the weighting function W_d, which will be discussed in the next section.

Remark 1 Unlike the traditional subspace predictor (13), the improved one (39) makes output prediction become a function of incremental input, i.e., Δu and therefore, an integral action will be imposed on the controller design procedure, which will be the solution for increasing the accuracy of reference tracking performance.

Remark 2 It should be mentioned that differentiating the I/O data may cause amplification of the measurement noises. In order to deal with this drawback, assuming that a priori knowledge about the characteristics of the noise is available, a pre-filter step is considered to reduce the effect of measurement noises by utilizing the inverse of the noise model (See Mardi and Wang (2008) for more details). This attempt can be classified as a preprocess step that should be made in data-driven controllers.

4 A Data-Driven Offset-Free $\mathscr{H}_\infty$ Controller

According to development in Chen et al. (2014), a solution is investigated to the problem (12) that gives a data-driven offset-free $\mathscr{H}_\infty$ controller.

The block diagram for the proposed controller is shown in Fig. 1 in which W_r, W_d and W_u are proper stable weighting functions that can be used as design parameters. According to this figure, plant's future output $\hat{y}$ is predicted using

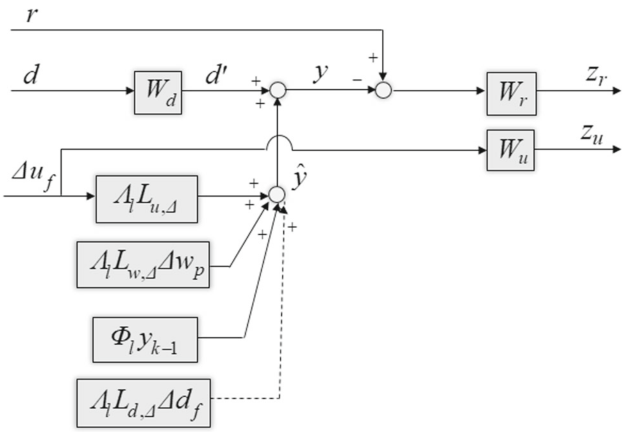

Fig. 1 The block diagram of data-driven offset-free $\mathscr{H}_\infty$ controller

the improved subspace predictor. Notice that the block with dashed arrow in Fig. 1 represents the additive component in (40), which will not be appeared in controller's design process and its effect will be compensated by W_d, which is a low-pass filter and demonstrates the relative importance along with the known or expected frequency substance of the external disturbance d_k. It should be pointed out that W_d plays an important role in disturbance attenuation purpose of the proposed controller and it is selected such that the effect of external disturbance be reduced on the system output. In other words, as discussed in the previous section, the effect of the external disturbance, which has been expressed as $\Lambda_l L_{d,\Delta} d_f$ in (40), is compensated by tuning of this weighting function. Control objectives are formed by coupling the weighting functions to the improved subspace predictor proposed in Sect. 3. W_r is chosen as a low-pass filter to reduce overshoots in system response, while W_u is chosen as a high-pass filter. Suppose state-space realizations of the weighting functions are as follows:

$$\mathbf{W_d}: \begin{cases} (x_{w_d})_{k+1} = A_{w_d}\,(x_{w_d})_k + B_{w_d}\,d_k \\ d'_k = C_{w_d}\,(x_{w_d})_k + D_{w_d}\,d_k \end{cases} \tag{41}$$

$$\mathbf{W_r}: \begin{cases} (x_{w_r})_{k+1} = A_{w_r}\,(x_{w_r})_k + B_{w_r}\,(r_k - y_k) \\ (z_r)_k = C_{w_r}\,(x_{w_r})_k + D_{w_r}\,(r_k - y_k) \end{cases} \tag{42}$$

$$\mathbf{W_u}: \begin{cases} (x_{w_u})_{k+1} = A_{w_u}\,(x_{w_u})_k + B_{w_u}\,\Delta u_k \\ (z_u)_k = C_{w_u}\,(x_{w_u})_k + D_{w_u}\,\Delta u_k \end{cases} \tag{43}$$

where k denotes the current time step. Consider Γ_r, Γ_d and Γ_u denote the extended observability matrices formed using impulse responses of the weighting functions as follows:

$$\Gamma_d = \begin{bmatrix} C_{w_d} \\ C_{w_d}\,A_{w_d} \\ \cdots \\ C_{w_d}\,A_{w_d}{}^{i-1} \end{bmatrix}, \ \Gamma_r = \begin{bmatrix} C_{w_r} \\ C_{w_r}\,A_{w_r} \\ \cdots \\ C_{w_r}\,A_{w_r}{}^{i-1} \end{bmatrix},$$

$$\Gamma_u = \begin{bmatrix} C_{w_u} \\ C_{w_u}\,A_{w_u} \\ \cdots \\ C_{w_u}\,A_{w_u}{}^{i-1} \end{bmatrix}$$

H_r, H_d and H_u denote lower triangular Toeplitz matrices formed using impulse responses of the weighting functions,

$$H_d \triangleq \begin{bmatrix} D_{w_d} & 0 & 0 & \cdots & 0 \\ C_{w_d}\,B_{w_d} & D_{w_d} & 0 & \cdots & 0 \\ C_{w_d}\,A_{w_d}\,B_{w_d} & C_{w_d}\,B_{w_d} & D_{w_d} & \cdots & 0 \\ \vdots & \vdots & \vdots & \ddots & \vdots \\ C_{w_d}\,A_{w_d}{}^{i-2}\,B_{w_d} & C_{w_d}\,A_{w_d}{}^{i-3}\,B_{w_d} & \cdots & C_{w_d}\,B_{w_d} & D_{w_d} \end{bmatrix}$$

$$H_r \triangleq \begin{bmatrix} D_{w_r} & 0 & 0 & \cdots & 0 \\ C_{w_r}\,B_{w_r} & D_{w_r} & 0 & \cdots & 0 \\ C_{w_r}\,A_{w_r}\,B_{w_r} & C_{w_r}\,B_{w_r} & D_{w_r} & \cdots & 0 \\ \vdots & \vdots & \vdots & \ddots & \vdots \\ C_{w_r}\,A_{w_r}{}^{i-2}\,B_{w_r} & C_{w_r}\,A_{w_r}{}^{i-3}\,B_{w_r} & \cdots & C_{w_r}\,B_{w_r} & D_{w_r} \end{bmatrix}$$

$$H_u \triangleq \begin{bmatrix} D_{w_u} & 0 & 0 & \cdots & 0 \\ C_{w_u}\,B_{w_u} & D_{w_u} & 0 & \cdots & 0 \\ C_{w_u}\,A_{w_u}\,B_{w_u} & C_{w_u}\,B_{w_u} & D_{w_u} & \cdots & 0 \\ \vdots & \vdots & \vdots & \ddots & \vdots \\ C_{w_u}\,A_{w_u}{}^{i-2}\,B_{w_u} & C_{w_u}\,A_{w_u}{}^{i-3}\,B_{w_u} & \cdots & C_{w_u}\,B_{w_u} & D_{w_u} \end{bmatrix}$$

then, using experimental I/O data, one has:

$$d' = \Gamma_d (x_{w_d})_k + H_d w \tag{44}$$

$$z_r = \Gamma_r (x_{w_r})_k + H_r (r - \hat{y} - d') \tag{45}$$

$$z_u = \Gamma_u (x_{w_u})_k + H_u \Delta u \tag{46}$$

where

$$w \triangleq \begin{bmatrix} w_k \\ w_{k+1} \\ \cdots \\ w_{k+i-1} \end{bmatrix}, \ \Delta u \triangleq \begin{bmatrix} \Delta u_k \\ \Delta u_{k+1} \\ \cdots \\ \Delta u_{k+i-1} \end{bmatrix}, \ \hat{y} \triangleq \begin{bmatrix} \hat{y}_k \\ \hat{y}_{k+1} \\ \cdots \\ \hat{y}_{k+i-1} \end{bmatrix},$$

$$z_r \triangleq \begin{bmatrix} (z_r)_k \\ (z_r)_{k+1} \\ \cdots \\ (z_r)_{k+i-1} \end{bmatrix}, \ z_u \triangleq \begin{bmatrix} (z_u)_k \\ (z_u)_{k+1} \\ \cdots \\ (z_u)_{k+i-1} \end{bmatrix}, \ d' \triangleq \begin{bmatrix} d'_k \\ d'_{k+1} \\ \cdots \\ d'_{k+i-1} \end{bmatrix}.$$

Theorem (1) summarizes the results:

Theorem 1 *If plant input measurements u, plant output measurements y, and reference signals r are available for time steps $k-i, \ldots, k-2, k-1$, therefore, the finite horizon, strictly causal, data-driven offset-free improved subspace-based level-γ, $\mathscr{H}_\infty$ controller for time steps $k, \ldots, k+i-1$ is obtained as*

$$\Delta u_{\text{opt}} = -(M_{22} - M_{12}^T M_{11}^{-1} M_{12})^{-1} \begin{bmatrix} -M_{12}^T M_{11}^{-1} & I \end{bmatrix} \times \left(\begin{bmatrix} M_{13} & M_{14} & M_{15} & M_{16} \\ M_{23} & M_{24} & M_{25} & M_{26} \end{bmatrix} \begin{bmatrix} \Delta w_p \\ x_{w_d} \\ x_{w_r} \\ x_{w_u} \end{bmatrix}_k + \begin{bmatrix} N_{11} \\ N_{21} \end{bmatrix} y_{k-1} \right) \tag{47}$$

Provided that

$$\gamma > \gamma_{\min}$$

where

$$\gamma_{\min} \triangleq \sqrt{\bar{\lambda}(M_{11_o} - M_{12}^T {M_{22}}^{-1} M_{12})}. \tag{48}$$

and

$$\begin{aligned}
&M_{11} = {H_w}^T H_w - \gamma^2 I, \quad M_{12} = -{H_w}^T H_r \Lambda_l L_{u,\Delta} \\
&M_{13} = -{H_w}^T H_r \Lambda_l L_{w,\Delta}, \quad M_{14} = -{H_w}^T H_r \Gamma_d, \\
&M_{15} = -{H_w}^T \Gamma_r, \quad M_{16} = 0, \\
&M_{22} = {L_{u,\Delta}}^T {\Lambda_l}^T {H_r}^T H_r \Lambda_l L_{u,\Delta} + {H_u}^T H_u, \\
&M_{23} = {L_{u,\Delta}}^T {\Lambda_l}^T {H_r}^T H_r \Lambda_l L_{w,\Delta}, \\
&M_{24} = {L_{u,\Delta}}^T {\Lambda_l}^T {H_r}^T H_r \Gamma_d, \\
&M_{25} = {L_{u,\Delta}}^T {\Lambda_l}^T {H_r}^T \Gamma_r, \quad M_{26} = {H_u}^T H_u, \\
&N_{11} = -{H_w}^T H_r \Phi_l, \quad N_{21} = {L_{u,\Delta}}^T {\Lambda_l}^T {H_r}^T H_r \Phi_l, \\
&M_{11_o} = M_{11} + \gamma^2 I,
\end{aligned}$$

Δu_{opt} is the vector of optimal incremental future inputs at time steps $k, \ldots, k+i-1$ as follows

$$\Delta u_{\text{opt}} = \begin{bmatrix} \Delta u_k \\ \vdots \\ \Delta u_{k+i-1} \end{bmatrix} \tag{49}$$

and the vector of optimal future inputs can be obtained by applying the following integral action:

$$u_{opt_k} = u_{opt_{k-1}} + \Delta u_{\text{opt}} \tag{50}$$

where $u_{opt_{k-1}} = \begin{bmatrix} u_{k-1} \\ u_k \\ \vdots \\ u_{k+i-2} \end{bmatrix}$ *and* $u_{opt_k} = \begin{bmatrix} u_k \\ u_{k+1} \\ \vdots \\ u_{k+i-1} \end{bmatrix}$.

Proof See "Appendix". □

It is worth noting that for non-zero reference signal inputs, the objective function utilized in Chen et al. (2014) does not meet zero steady-state tracking error, unless the open-loop system possesses an integral action (Kadali et al. 2003; Shafiei et al. 2015). Thereupon, by taking the integrated noise model into account, the I/O data are differentiated and an integrator is incorporated into the proposed controller. Strictly speaking, the modified objective function (56) becomes a function of incremental input. Notice that (50) contains a guaranteed integrator. Designing steps of the proposed controller are summarized by the following algorithm:

Algorithm 1 *Data-Driven Offset-free $\mathscr{H}_\infty$ Controller Design*

1. *Collect experimental I/O data from the unknown healthy LTI system (5) and differentiate it.*
2. *Define differentiated Hankel matrices ΔU_p, ΔY_p, ΔU_f, ΔY_f according to (24)–(27).*
3. *Form ΔW_p using (28).*
4. *Compute $L_{u,\Delta}$ and $L_{w,\Delta}$ regarding Eqs. (30) and (31).*
5. *Choose weighting functions W_r, W_d and W_u.*
6. *Calculate $\gamma_{\min}$ using (48) and choose $\gamma > \gamma_{\min}$.*
7. *Initialize states of weighting functions (x_{w_r}, x_{w_d} and x_{w_u}) using (41)–(43).*
8. *Form Δw_{p_k} according to (35).*
9. *Compute Δu_{opt} for current time step k according to (47).*
10. *Apply first time step of Δu_{opt} and take measurements y_k (real system output) and r_k.*
11. *Update states of weighting functions.*
12. *$k := k + 1$ and go to Step 8.*

Steps 8–12 should be repeated i times.

Remark 3 By selecting less value for γ, better results are obtained in control objectives. However, as noticed in Woodley et al. (2001), choosing γ nearby $\gamma_{\min}$ can cause control objectives not met. Because the formula used for calculating Δu_{opt} is close to singularity near $\gamma_{\min}$. Hence, it is better to choose $\gamma \geq 1.1\gamma_{\min}$ in which $\gamma_{\min}$ is calculated according to equation (48).

Remark 4 Due to the fact that determination of precise subspace predictor is necessary for desired closed-loop performance, the richness and frequency content of I/O data are significantly important in order to excite all modes of the plant and capture its real behavior. Hence, quality of the I/O data should be ensured. In the other hand, length of the I/O data is another term that affects the performance of the predictor. The subspace-based predictor derived utilizing short length of I/O data will not be able to favorably capture the plant's dynamic behavior. Therefore, an accurate predictor can be obtained by longer length of I/O data. Meanwhile, the sampling frequency should be chosen well above the plant's cut-off frequency in order to capture all modes of the plant and obtain a satisfactory predictor.

Remark 5 The main constraint of the subspace-based controllers is the stability of the open-loop system. Acquiring I/O data from the open-loop plant is required for the step of computing predictor's coefficients. Unstable plant will generate unbounded output data, which are useless for determination of subspace-based predictors. Designing simple and low-cost controllers such as proportional–integral–derivative (PID) controller as an inner loop for stabilizing the open-loop system is one of the solutions. In other words, for unstable systems, the I/O data is collected from the inner closed-loop system instead of the open-loop one.

5 Numerical Examples

In this section, to verify the effectiveness of the theoretical results, Algorithm 1 and the method of Chen et al. (2014), which will be referred as Chen's method for convenience, are applied to the following numerical examples by means of MATLAB/Simulink and the results are compared. Notice that, in order to illustrate the effect of considering W_d in design procedure and emphasize the superior robustness of the proposed study, an external disturbance, i.e., d_k, is considered to perturb the plants. It should be mentioned that the weighting function W_d has not been considered in Chen's method.

5.1 Example 1

Consider the following LTI system:

$$G: \begin{cases} \dot{x} = \begin{bmatrix} -49.2 & -1.3 \\ 59.04 & -2.5 \end{bmatrix} x + \begin{bmatrix} 190.4 \\ 0 \end{bmatrix} u \\ \qquad + \begin{bmatrix} 0 \\ -54.26 \end{bmatrix} d + \xi \\ y = \begin{bmatrix} 0 & 1 \end{bmatrix} x + \vartheta \end{cases} \tag{51}$$

where $x = \begin{bmatrix} x_1 & x_2 \end{bmatrix}^T$ is system state vector. I/O data are collected by applying pseudo random binary sequence (PRBS) to the system (51) and recording its output with sampling frequency of 200 Hz, $N = 2000$ and $i = 55$. Figure 2a and b respectively show the PRBS input and the response of the system (51), which are used for evaluating the coefficients of both traditional and improved subspace predictors. Notice that output data are distributed by an integrated noise with signal to noise ratio (SNR) of 20 db. As mentioned in Sect. 3, in traditional subspace predictor, we use normal data, while differentiated data are used for improved one. The weighting transfer functions are chosen in continuous domain as follows and discretized by tustin transform:

$$W_r = \frac{0.01(s+10)}{(s+0.01)},\ W_d = \frac{0.1(s+10)}{(s+0.01)},\ W_u = \frac{10(s+0.01)}{(s+10)}$$

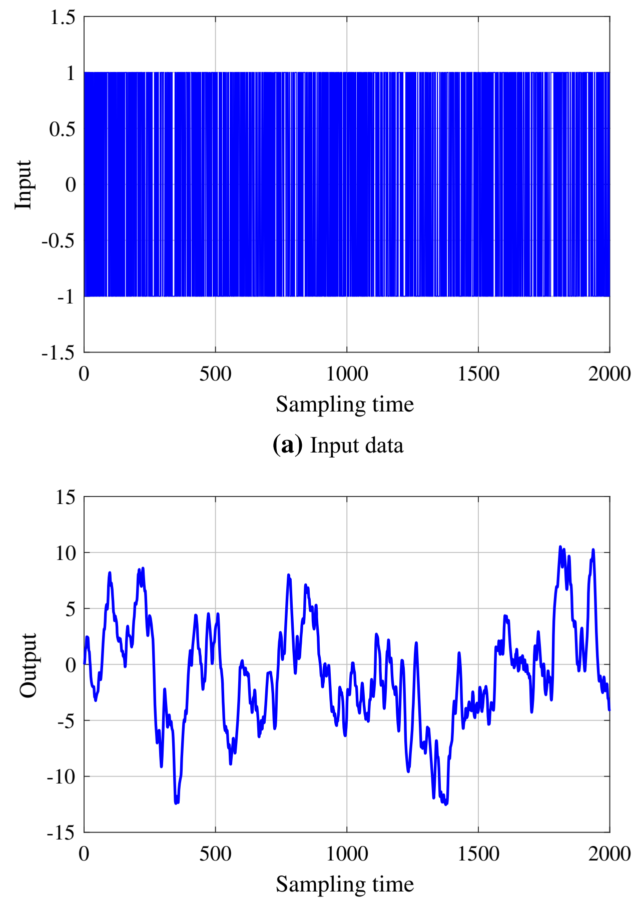

(a) Input data

(b) Output data

Fig. 2 I/O data collected from system in example 1

As mentioned above, the control objective is to force the system state to track a desired signal, while attenuating the effect of external disturbance. For this issue, consider the reference signal and the disturbance as follows:

$$r(t) = \begin{cases} 0, & t < 10 \\ 2, & 10 \le t < 77 \\ 1.5, & 77 \le t \end{cases}$$

and

$$d(t) = \begin{cases} 0, & t < 37 \\ 1.5, & 37 \le t < 56 \\ 0, & 56 \le t \end{cases}$$

Figure 3 compares the tracking performance of the proposed study with that of Chen's method. Evidently, one can see the tracking performance of the proposed controller is offset-free, while the compared work has a significant steady-state tracking error and the output response of the proposed work tracks the reference signal faster. It can be seen that when the external disturbance perturbs the system during the time

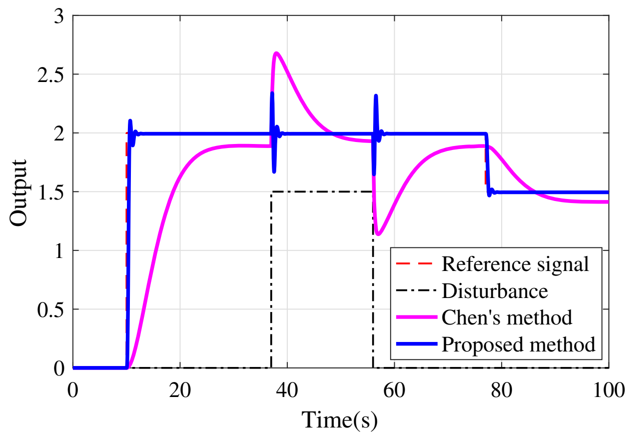

Fig. 3 Comparison of trajectory tracking performance of example 1

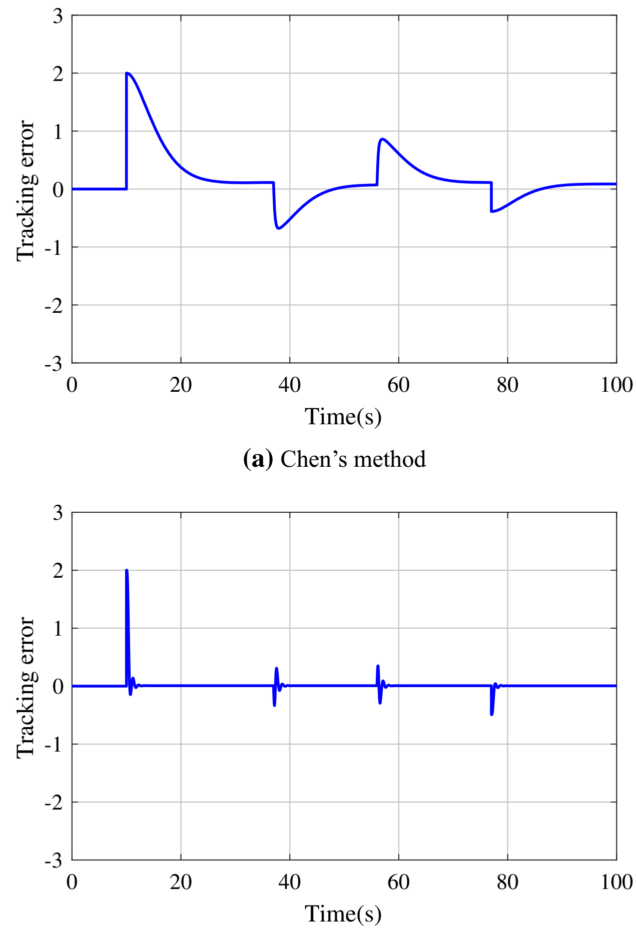

(a) Chen's method

(b) Proposed method

Fig. 4 Tracking error of example 1

interval of 37 to 56 s, the proposed controller quickly attenuates its effect because of the weight function, i.e., W_d, has been used in the controller's design procedure to compensate the effect of the external disturbance. Furthermore, the output response has less overshoot than that of Chen's method. Therefore, the proposed controller has more robustness. Considering the tracking error results in Fig. 4a and b, performance indexes including the integral of the absolute error (IAE), the integral of the square error (ISE) and the integral of the time multiplied by the absolute error (ITAE) (Hsiao et al. 2008) have been calculated for quantitative comparison and listed in Table 1, which emphasizes better tracking performance of our work.

The control efforts of both works are demonstrated in Fig. 5a and b. It is worth mentioning that the proposed control input is more aggressive than that of Chen's method, which is reasonable due to its fast offset-free tracking and disturbance attenuating performance. Nevertheless, it has not abrupt and fast changes, which has been emphasized in Fig. 5b.

Table 1 Tracking performance comparison of example 1

Controller	IAE	ISE	ITAE
Chen's method	27.40	22.25	1.039×10^3
Proposed method	1.93	1.33	0.071×10^3

5.2 Example 2

In this subsection, another simulation study is accomplished in order to demonstrate the performance of the proposed study. Consider the discrete-time process of injection molding (IM) as follows:

$$G : \begin{cases} x_{k+1} = \begin{bmatrix} 1.582 & -0.592 \\ 1 & 0 \end{bmatrix} x_k + \begin{bmatrix} 1 \\ 0 \end{bmatrix} (u_k + d_k) + \xi_k \\ y_k = \begin{bmatrix} 1.69 & 1.419 \end{bmatrix} x_k + \vartheta_k \end{cases} \tag{52}$$

where $d_k = \left((-0.15z^{-1} - 0.2z^{-2})/(1 - 0.993z^{-1})\right)\delta_{k-k_0}$ is the external disturbance shown in Fig. 6 and $\delta_{k-k_0} = 0.01$. $k_0 = 6600$ and according to the sampling frequency, i.e., 200 Hz, it is equal to 33th second in the time interval of simulation. In other words, in 33th second of simulation, d_k perturbs the process. The interested readers can refer to Hou et al. (2018) for more details about this process. I/O data are acquired by applying pseudo random binary sequence (PRBS) to the system (52), which are used to compute the coefficients of both traditional and improved subspace predictors. $i = 10$ and the other parameters are selected as those of example 1. The weighting transfer functions are chosen in continuous domain as follows and discretized by tustin transform:

$$W_r = \frac{0.01(s+5)}{(s+0.01)},\ W_d = \frac{0.1(s+5)}{(s+0.01)},\ W_u = \frac{10(s+0.01)}{(s+5)}$$

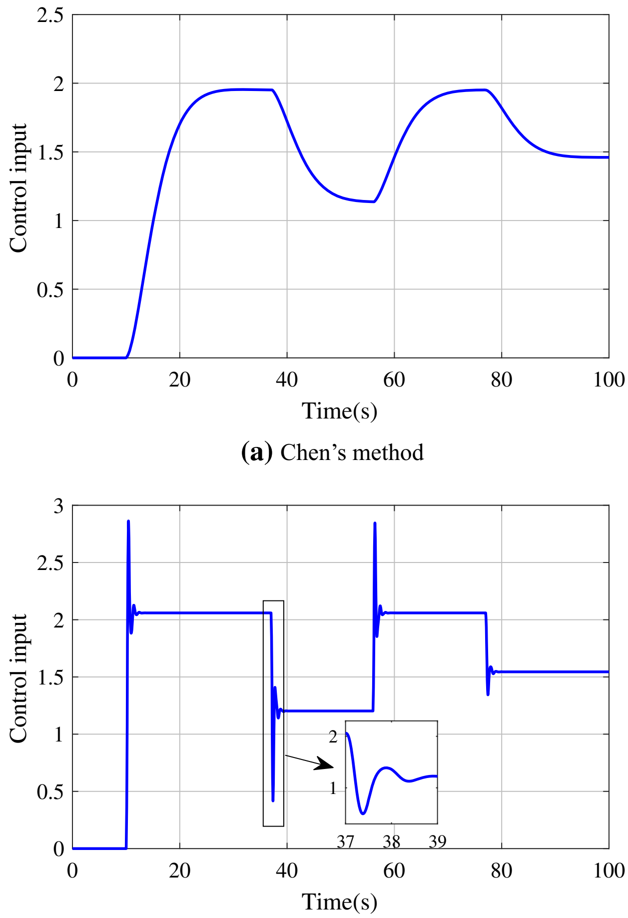

(a) Chen's method

(b) Proposed method

Fig. 5 Control input of example 1

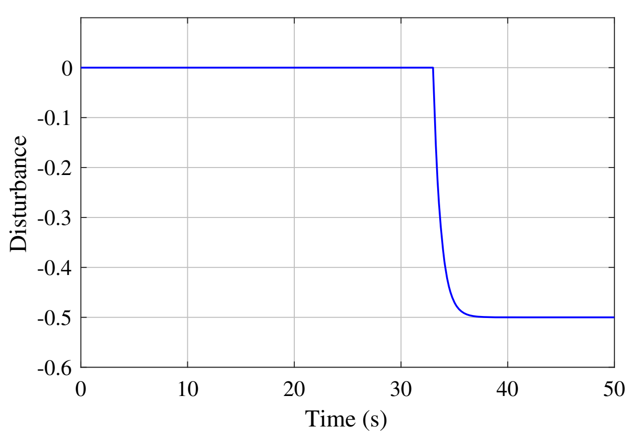

Fig. 6 Disturbance of example 2

To challenge the tracking performance of the proposed study, a time-variant reference signal is given as follows:

$$r(k+1)=\begin{cases} 50\times(-1)^{\mathrm{round}(k/2000)}+70, & k\le 4001 \\ \big(50\sin(k\pi/1000)+ \\ 20\cos(k\pi/500)+70\big), & 4001<k\le 6001 \\ 50\times(-1)^{\mathrm{round}(k/2000)}+70, & 6001<k\le 1000 \end{cases}$$

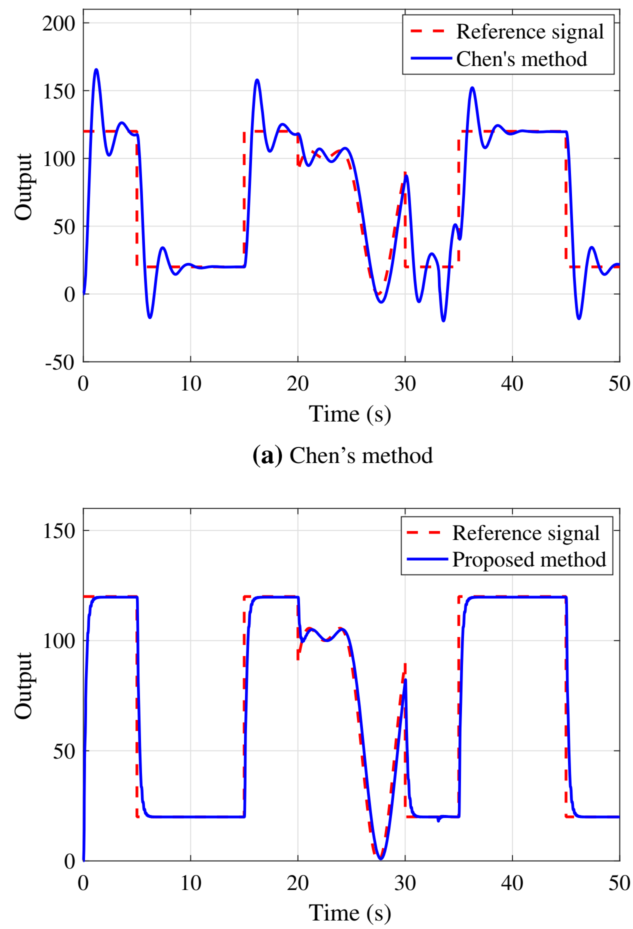

(a) Chen's method

(b) Proposed method

Fig. 7 Tracking performance comparison of example 2

For comparison purpose, Chen's method is also implemented on IM process and the compared results are illustrated in Figs. 7 and 8. Regarding Fig. 7, more accurate tracking performance of the proposed controller is deduced. In contrast to the proposed method, the system output of Chen's method has undesired overshoots. In addition, the robustness of the proposed controller has been improved due to the weighting function W_d has been considered in design procedure. For quantitative comparison, the root mean square of the tracking error is computed and listed in Table 2. According to this table, better tracking performance of the proposed controller is concluded.

Finally, Fig. 8 displays both methods' control signals. The proposed controller has more aggressive control signal in order to provide more accurate tracking performance. However, it is smooth and sensible as emphasized in Fig. 8b.

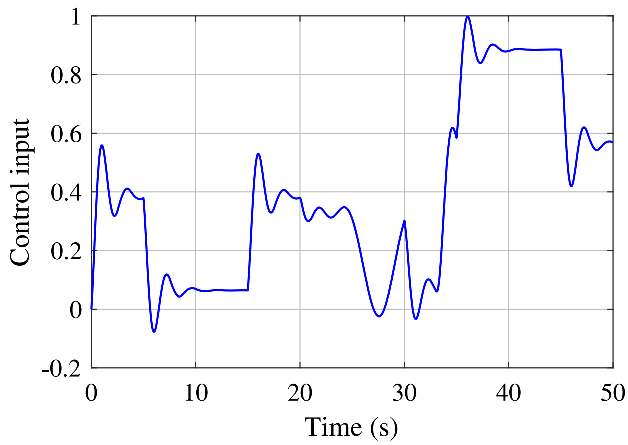

(a) Chen's method

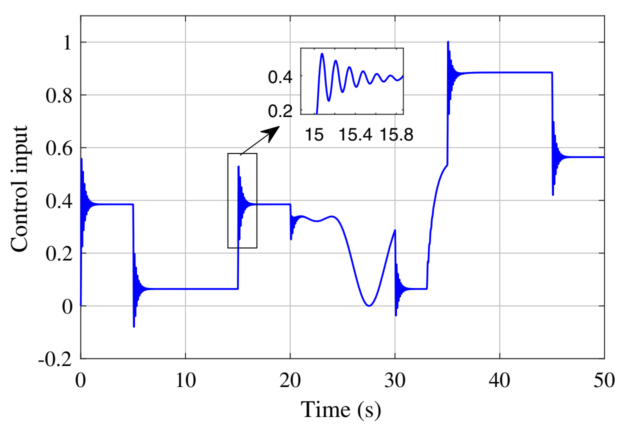

(b) Proposed method

Fig. 8 Control input of example 2

Table 2 Tracking performance comparison of example 2

Controller	RMS
Chen's method	23.30
Proposed method	13.11

6 Conclusion

This paper, addresses the problem of accurate reference tracking performance in presence of external disturbances using data-driven $\mathscr{H}_\infty$ controller. Merely using the I/O data, the improved subspace-predictor is formulated to predict the plant outputs. In contrast with the traditional subspace predictor, the improved one imposes an integral action to the control loop to enhance the tracking accuracy. A low-pass filter as a weighting function is also considered to attenuate the effect of external disturbances. The effectiveness of the proposed study is demonstrated by means of simulations, and the comparative results indicate its superiority. The extension of the proposed work for unknown nonlinear systems will be our future work.

Appendix

Proof of Theorem 1: Calculate $\hat{y}$ using improved subspace predictor (39) using differentiated I/O data collected from the unknown healthy system (15). Substituting (13) and (44) into (45), one can get

$$z_c = \begin{bmatrix} z_r \\ z_u \end{bmatrix} = \begin{bmatrix} \Gamma_r (x_{w_r})_k + H_w w - H_r \Gamma_d (x_{w_d})_k \\ \Gamma_u (x_{w_u})_k + H_u \, \Delta u_k \end{bmatrix} + \begin{bmatrix} -H_r \, \Lambda_l \, L_{u,\Delta} \, \Delta u - H_r \, \Lambda_l \, L_{w,\Delta} \, \Delta(w_p)_k - H_r \, \Phi_l \, y_{k-1} \\ 0 \end{bmatrix} \tag{53}$$

where

$$H_w \triangleq H_r K_{\text{ref}} - H_r H_d K_{\text{dist}}$$

and

$$K_{\text{ref}} \triangleq \begin{bmatrix} K_1 & 0 & \cdots & 0 \\ 0 & K_1 & \cdots & 0 \\ \vdots & 0 & \ddots & 0 \\ 0 & 0 & \cdots & K_1 \end{bmatrix}, \quad K_{\text{dist}} \triangleq \begin{bmatrix} K_2 & 0 & \cdots & 0 \\ 0 & K_2 & \cdots & 0 \\ \vdots & 0 & \ddots & 0 \\ 0 & 0 & \cdots & K_2 \end{bmatrix}$$

Defining

$$X^T = \left[w^T \;\; \Delta u_k{}^T \;\; \Delta w_{p_k}{}^T \;\; x_{w_{d\,k}}{}^T \;\; x_{w_{r\,k}}{}^T \;\; x_{w_{u\,k}}{}^T \right] \tag{54}$$

we have

$$z_c = \underbrace{\begin{bmatrix} H_w & -H_r \, \Lambda_l \, L_{u,\Delta} & -H_r \, \Lambda_l \, L_{w,\Delta} & -H_r \, \Gamma_d & \Gamma_r & 0 \\ 0 & H_u & 0 & 0 & 0 & \Gamma_u \end{bmatrix}}_{\Omega} X + \underbrace{\begin{bmatrix} -H_r \, \Phi_l \\ 0 \end{bmatrix}}_{\Psi} y_{k-1} \tag{55}$$

Substituting (55) into (10) yields

$$J = X^T \underbrace{\Omega^T \Omega}_{M} X + X^T \underbrace{\Omega^T \Psi}_{N} y_{k-1} + y_{k-1}{}^T \Psi^T \Omega X + y_{k-1}{}^T \Psi^T \Psi y_{k-1}$$

where

$$M = \begin{bmatrix} M_{11} & M_{12} & M_{13} & M_{14} & M_{15} & M_{16} \\ M_{21} & M_{22} & M_{23} & M_{24} & M_{25} & M_{26} \\ M_{31} & M_{32} & M_{33} & M_{34} & M_{35} & M_{36} \\ M_{41} & M_{42} & M_{43} & M_{44} & M_{45} & M_{46} \\ M_{51} & M_{52} & M_{53} & M_{54} & M_{55} & M_{56} \\ M_{61} & M_{62} & M_{63} & M_{64} & M_{65} & M_{66} \end{bmatrix}, \; N = \begin{bmatrix} N_{11} \\ N_{21} \\ N_{31} \\ N_{41} \\ N_{51} \\ N_{61} \end{bmatrix}$$

and

$$
\begin{aligned}
&M_{21} = {M_{12}}^T,\\
&M_{31} = {M_{13}}^T, \quad M_{32} = {M_{23}}^T,\\
&M_{33} = {L_{w,\Delta}}^T\, {\Lambda_l}^T\, {H_r}^T\, H_r\, \Lambda_l\, L_{w,\Delta},\\
&M_{34} = {L_{w,\Delta}}^T\, {\Lambda_l}^T\, {H_r}^T\, H_r\, \Gamma_d,\\
&M_{35} = {L_{w,\Delta}}^T\, {\Lambda_l}^T\, {H_r}^T\, \Gamma_r, \quad M_{36} = 0,\\
&M_{41} = {M_{14}}^T, \quad M_{42} = {M_{24}}^T,\\
&M_{43} = {M_{34}}^T, \quad M_{44} = {\Gamma_d}^T\, {H_r}^T\, H_r\, \Gamma_d,\\
&M_{45} = {\Gamma_d}^T\, {H_r}^T\, H_r\, \Gamma_r, \quad M_{46} = 0,\\
&M_{51} = {M_{15}}^T, \quad M_{52} = {M_{25}}^T,\\
&M_{53} = {M_{35}}^T, \quad M_{54} = {M_{45}}^T,\\
&M_{55} = {\Gamma_r}^T\, \Gamma_r, \quad M_{56} = 0,\\
&M_{61} = {M_{16}}^T, \quad M_{62} = {M_{26}}^T,\\
&M_{63} = {M_{36}}^T, \quad M_{64} = {M_{46}}^T,\\
&M_{65} = {M_{46}}^T, \quad M_{66} = {\Gamma_u}^T\, \Gamma_u,\\
&N_{31} = {L_{w,\Delta}}^T\, {\Lambda_l}^T\, {H_r}^T\, H_r\, \Phi_l, \quad N_{41} = {\Gamma_d}^T\, {H_r}^T\, H_r\, \Phi_l,\\
&N_{51} = -{\Gamma_r}^T\, H_r\, \Phi_l, \quad N_{61} = 0.
\end{aligned}
$$

and M_{1i}, M_{2i} $(i = 1, \ldots, 6)$ and N_{11}, N_{21} were defined in Theorem 1. Hence, Eq. (12) is written as

$$
\begin{aligned}
&\min_{\Delta u} \sup_{w} \,(X^T M X + X^T N y_{k-1} + {y_{k-1}}^T N^T X\\
&\quad + {y_{k-1}}^T \Psi^T \Psi\, y_{k-1}) \leq 0
\end{aligned}
\tag{56}
$$

Solve the following equation

$$
\frac{\partial J}{\partial \begin{bmatrix} w \\ \Delta u \end{bmatrix}} = 0,
$$

which gives the optimal Δu and the worst case w, i.e., w_{wc} as follows

$$
\begin{aligned}
\begin{bmatrix} w_{wc} \\ \Delta u_{\text{opt}} \end{bmatrix} &= -\begin{bmatrix} M_{11} & M_{12} \\ M_{21} & M_{22} \end{bmatrix}^{-1}\\
&\times \left(\begin{bmatrix} M_{13} & M_{14} & M_{15} & M_{16} \\ M_{23} & M_{24} & M_{25} & M_{26} \end{bmatrix} \begin{bmatrix} \Delta w_p \\ x_{w_d} \\ x_{w_r} \\ x_{w_u} \end{bmatrix} + \begin{bmatrix} N_{11} \\ N_{21} \end{bmatrix} y_{k-1} \right)
\end{aligned}
\tag{57}
$$

Defining

$$
H_{hess} \triangleq \frac{\partial^2 J}{\partial^2 \begin{bmatrix} w \\ \Delta u \end{bmatrix}} = \begin{bmatrix} M_{11} & M_{12} \\ M_{21} & M_{22} \end{bmatrix} = \begin{bmatrix} A_1 & A_2 \\ {A_2}^T & A_3 \end{bmatrix}
$$

and using lemma (2), one has

$$
H_{hess} = \Upsilon^T Q \Upsilon,
$$

where

$$
\Upsilon = \begin{bmatrix} I & 0 \\ {A_3}^{-1}{A_2}^T & I \end{bmatrix}, \; Q = \begin{bmatrix} A_1 - A_2 {A_3}^{-1} {A_2}^T & 0 \\ 0 & A_3 \end{bmatrix}
$$

The sufficient (saddle) condition of optimization is that matrix Q must have $(k_d + l)i$ positive and mi negative eigenvalues. Since, $A_3 > 0$, therefore, it provides aforementioned positive eigenvalues. So the sufficient condition reduces to $A_1 - A_2 {A_3}^{-1} {A_2}^T < 0$. Then

$$
\begin{aligned}
&M_{11} - M_{12} {M_{22}}^{-1} {M_{12}}^T < 0,\\
&M_{11o} - M_{12}^T\, {M_{22}}^{-1}\, M_{12} < \gamma^2 I,\\
&\gamma_{\min} < \gamma,
\end{aligned}
$$

where

$$
\gamma_{\min} = \sqrt{\bar{\lambda}(M_{11o} - M_{12}^T\, {M_{22}}^{-1}\, M_{12})},
$$

The proof is completed.

References

Cheng, L., Liu, W., Hou, Z. G., Yu, J., & Tan, M. (2015). Neural-network-based nonlinear model predictive control for piezoelectric actuators. *IEEE Transactions on Industrial Electronics*, *62*(12), 7717–7727.

Chen, J., Yang, F., & Han, Q. L. (2014). Model-free predictive $\mathscr{H}_\infty$ control for grid-connected solar power generation systems. *IEEE Transactions on Control Systems Technology*, *22*(5), 2039–2047.

Elkaim, G. H., Woodley, B. R., & Kelbley, R. J. (2006). Model free subspace H control for an autonomous catamaran. In *2006 IEEE/ION position, location, and navigation symposium* (pp. 1005–1013). IEEE.

Errouissi, R., Al-Durra, A., & Muyeen, S. (2016). Offset-free feedback linearisation control of a three-phase grid-connected photovoltaic system. *IET Power Electronics*, *9*(9), 1933–1942.

Esmaeili, B., Baradarannia, M., Salim, M., & Farzamnia, A. (2019a). Data-driven MIMO discrete-time predictive model-free adaptive integral terminal sliding mode controller design for robotic manipulators driven by pneumatic artificial muscles. In *2019 6th international conference on control, instrumentation and automation (ICCIA)* (pp. 1–8). IEEE.

Esmaeili, B., Beyramzad, J., Seyyedrasuli, M., Noorani, M. R. S., & Ghanbari, A. (2018). Using fuzzy neural network sliding mode control for human–exoskeleton interaction forces minimization. In *2018 IEEE international conference on mechatronics and automation (ICMA)* (pp. 403–410). IEEE.

Esmaeili, B., Salim, M., Baradarannia, M., & Farzamnia, A. (2019b). Data-driven observer-based model-free adaptive discrete-time terminal sliding mode control of rigid robot manipulators. In *2019 7th international conference on robotics and mechatronics (ICRoM)* (pp. 432–438). IEEE.

Favoreel, W., De Moor, B., Van Overschee, P., & Gevers, M. (1999). Model-free subspace-based LQG-design. In *Proceedings of the 1999 American control conference (Cat. No. 99CH36251)* (vol. 5, pp. 3372–3376). IEEE.

Ge, S. S., Hang, C. C., Lee, T. H., & Zhang, T. (2013). *Stable adaptive neural network control* (Vol. 13). Berlin: Springer.

Hallouzi, R., & Verhaegen, M. (2008). Fault-tolerant subspace predictive control applied to a Boeing 747 model. *Journal of Guidance, Control, and Dynamics*, *31*(4), 873–883.

Heertjes, M. F., Van der Velden, B., & Oomen, T. (2016). Constrained iterative feedback tuning for robust control of a wafer stage system. *IEEE Transactions on Control Systems Technology*, *24*(1), 56–66.

Hou, J., Liu, T., & Wang, Q. G. (2018). Recursive subspace identification subject to relatively slow time-varying load disturbance. *International Journal of Control*, *91*(3), 622–638.

Hou, Z. S., & Wang, Z. (2013). From model-based control to data-driven control: Survey, classification and perspective. *Information Sciences*, *235*, 3–35.

Houtzager, I., van Wingerden, J. W., & Verhaegen, M. (2012). Recursive predictor-based subspace identification with application to the real-time closed-loop tracking of flutter. *IEEE Transactions on Control Systems Technology*, *20*(4), 934–949.

Hsiao, M. Y., Li, T. H. S., Lee, J. Z., Chao, C. H., & Tsai, S. H. (2008). Design of interval type-2 fuzzy sliding-mode controller. *Information Sciences*, *178*(6), 1696–1716.

Kadali, R., Huang, B., & Rossiter, A. (2003). A data driven subspace approach to predictive controller design. *Control Engineering Practice*, *11*(3), 261–278.

Katayama, T. (2006). *Subspace methods for system identification*. Berlin: Springer.

Khajehsaeid, H., Esmaeili, B., Soleymani, R., & Delkhosh, A. (2019). Adaptive back stepping fast terminal sliding mode control of robot manipulators actuated by pneumatic artificial muscles: continuum modelling, dynamic formulation and controller design. *Meccanica*, *54*(8), 1203–1217.

Li, Z., Deng, J., Lu, R., Xu, Y., Bai, J., & Su, C. Y. (2016). Trajectory-tracking control of mobile robot systems incorporating neural-dynamic optimized model predictive approach. *IEEE Transactions on Systems, Man, and Cybernetics: Systems*, *46*(6), 740–749.

Lu, X., Chen, H., Gao, B., Zhang, Z., & Jin, W. (2015). Data-driven predictive gearshift control for dual-clutch transmissions and FPGA implementation. *IEEE Transactions on Industrial Electronics*, *62*(1), 599–610.

Lu, X., Chen, H., Wang, P., & Gao, B. (2011). Design of a data-driven predictive controller for start-up process of amt vehicles. *IEEE Transactions on Neural Networks*, *22*(12), 2201–2212.

Luo, X. S., & Song, Y. D. (2018). Data-driven predictive control of Hammerstein–Wiener systems based on subspace identification. *Information Sciences*, *422*, 447–461.

Mardi, N. A., & Wang, L. (2008). Subspace-based model predictive control with data prefiltering. In *Proceedings of the UKACC international conference on control*, Manchester, UK.

Mardi, N. A., & Wang, L. (2009). Subspace-based model predictive control of time-varying systems. In *Proceedings of the 48th IEEE conference on decision and control, 2009 held jointly with the 2009 28th Chinese control conference* (pp. 4005–4010). CDC/CCC 2009. IEEE.

Markovsky, I., Willems, J. C., Rapisarda, P., & De Moor, B. L. (2005). Data driven simulation with applications to system identification. *IFAC Proceedings Volumes*, *38*(1), 970–975.

Precup, R. E., & Hellendoorn, H. (2011). A survey on industrial applications of fuzzy control. *Computers in Industry*, *62*(3), 213–226.

Salim, M., & Khosrowjerdi, M. (2016). An $\mathscr{H}_\infty$ approach to data-driven simultaneous fault detection and control. *IMA Journal of Mathematical Control and Information*, *34*(4), 1195–1213.

Salim, M., & Khosrowjerdi, M. J. (2017). Data-driven $\mathscr{H}_\infty$ controller/detector design for a quadruple tank process. *Journal of Control Engineering and Applied Informatics*, *19*(1), 3–14.

Shafiei, S. E., Knudsen, T., Wisniewski, R., & Andersen, P. (2015). Data-driven predictive direct load control of refrigeration systems. *IET Control Theory & Applications*, *9*(7), 1022–1033.

Vajpayee, V., Mukhopadhyay, S., & Tiwari, A. P. (2018). Data-driven subspace predictive control of a nuclear reactor. *IEEE Transactions on Nuclear Science*, *65*(2), 666–679.

Van Overschee, P., & De Moor, B. (1994). N4SID: Subspace algorithms for the identification of combined deterministic-stochastic systems. *Automatica*, *30*(1), 75–93.

Van Overschee, P., & De Moor, B. (1996). *Subspace identification for linear systems: Theory-implementations-applications*. Berlin: Springer.

Van, M. (2019). Adaptive neural integral sliding-mode control for tracking control of fully actuated uncertain surface vessels. *International Journal of Robust and Nonlinear Control*, *29*(5), 1537–1557.

Wahab, N., Katebi, R., Balderud, J., & Rahmat, M. (2011). Data-driven adaptive model-based predictive control with application in wastewater systems. *IET Control Theory & Applications*, *5*(6), 803–812.

Woodley, B. R., How, J. P., & Kosut, R. L. (2001a). Model free subspace based $\mathscr{H}_\infty$ control. In *Proceedings of the 2001 American control conference, 2001* (vol. 4, pp. 2712–2717). IEEE.

Woodley, B. R., How, J. P., & Kosut, R. L. (2001b). Subspace based direct adaptive $\mathscr{H}_\infty$ control. *International Journal of Adaptive Control and Signal Processing*, *15*(5), 535–561.

Wu, X., Shen, J., Li, Y., & Lee, K. Y. (2014). Data-driven modeling and predictive control for boiler-turbine unit using fuzzy clustering and subspace methods. *ISA Transactions*, *53*(3), 699–708.

Yan, P., Liu, D., Wang, D., & Ma, H. (2016). Data-driven controller design for general mimo nonlinear systems via virtual reference feedback tuning and neural networks. *Neurocomputing*, *171*, 815–825.